Electrochemical and Spectral Characterization of Iron Corroles in High and Low Oxidation States: First Structural Characterization of an Iron(IV) Tetrapyrrole π Cation Radical

Eric Van Caemelbecke,[†] Stefan Will,[‡] Marie Autret,[†] Victor A. Adamian,[†] Johann Lex,[‡] Jean-Paul Gisselbrecht,[§] Maurice Gross,*[,§] Emanuel Vogel,*[,‡] and Karl M. Kadish*[,†]

Department of Chemistry, University of Houston, Houston, Texas 77204-5641, Institut für Organische Chemie, Universität zu Köln, Greinstrasse 4, D-50939 Köln, Germany, and Département de Chimie, URA CNRS 405, Université Louis Pasteur, 67000 Strasbourg, France

Received July 14, 1995[⊗]

The electrochemistry and spectroscopic properties of three iron corroles were examined in benzonitrile, dichloromethane, and pyridine containing 0.1 M tetra-*n*-butylammonium perchlorate or tetra-*n*-ethylammonium hexafluorophosphate as supporting electrolyte. The investigated compounds are represented as (OEC)$Fe^{IV}(C_6H_5)$, (OEC)Fe^{IV}Cl, and (OEC)Fe^{III}(py), where OEC is the trianion of 2,3,7,8,12,13,17,18-octaethylcorrole. Each iron(IV) corrole undergoes two one-electron reductions and two or three one-electron oxidations depending upon the solvent. Under the same solution conditions, the iron(III) corrole undergoes a single one-electron reduction and one or two one-electron oxidations. Each singly oxidized and singly reduced product was characterized by UV−vis and/or EPR spectroscopy. The data indicate a conversion of (OEC)$Fe^{IV}(C_6H_5)$ and (OEC)Fe^{IV}Cl to their iron(III) forms upon a one-electron reduction and to iron(IV) corrole π cation radicals upon a one-electron oxidation. The metal center in $[(OEC)Fe^{III}(C_6H_5)]^-$ is low spin ($S = {}^1/_2$) as compared to electrogenerated $[(OEC)Fe^{III}Cl]^-$, which contains an intermediate-spin ($S = {}^3/_2$) iron(III). (OEC)Fe^{III}(py) also contains an intermediate-spin-state iron(III) and, unlike previously characterized (OEC)Fe^{III}(NO), is converted to an iron(IV) corrole upon oxidation rather than to an iron(III) π cation radical. Singly oxidized $[(OEC)Fe^{IV}(C_6H_5)]^{\bullet+}$ is the first iron(IV) tetrapyrrole π cation radical to be isolated and was structurally characterized as a perchlorate salt. It crystallizes in the triclinic space group $P\bar{1}$ with $a = 10.783(3)$ Å, $b = 13.826(3)$ Å, $c = 14.151(3)$ Å, $\alpha = 78.95(2)°$, $\beta = 89.59(2)°$, and $\gamma = 72.98(2)°$ at 293 K with $Z = 2$. Refinement of 8400 reflections and 670 parameters against F_o^2 yields R1 = 0.0864 and wR2 = 0.2293. The complex contains a five-coordinated iron with average Fe−N bond lengths of 1.871(3) Å. The formulation of the electron distribution in this compound was confirmed by Mössbauer, X-ray crystallographic, and magnetic susceptibility data as well as by EPR spectroscopy, which gives evidence for strong antiferromagnetic coupling between the iron(IV) center and the singly oxidized corrole macrocycle.

Introduction

The chemical or electrochemical oxidation of synthetic iron(III) porphyrins and related macrocycles can lead to iron(IV) derivatives or to iron(III) π cation radicals depending upon the initial spin state and the nature of the axial ligand.[1−24] Oxo,[2,4,6,7,10,19] alkoxy,[6,7,10] hydroxy,[10,11,14,16,19,20] or σ-bonded[3,17] phenyl axial ligands seem to be crucial in generation of monomeric iron porphyrins in a +4 oxidation state in solutions, but none of these porphyrins have been isolated and structurally characterized. Until recently, the only structurally characterized macrocyclic iron(IV) complex was a species with a tetraamide ligand which possessed a −4 charge and was thus able to stabilize a higher oxidation state of the central metal ion.[23] However, the preparation and structural characterization of (OEC)$Fe^{IV}(C_6H_5)$ and (OEC)Fe^{IV}Cl, where OEC is the trianion

[†] University of Houston.
[‡] Universität zu Köln.
[§] Université Louis Pasteur.
[⊗] Abstract published in *Advance ACS Abstracts,* November 1, 1995.

(1) Chin, D.-H.; Balch, A. L.; La Mar, G. N. *J. Am. Chem. Soc.* **1980**, *102*, 1446.
(2) Balch, A. L.; Chan, Y.-W.; Cheng, R.-J.; La Mar, G. N.; Latos-Grazynski, L.; Renner, M. W. *J. Am. Chem. Soc.* **1984**, *106*, 7779.
(3) Lançon, D.; Cocolios, P.; Guilard, R.; Kadish, K. M. *J. Am. Chem. Soc.* **1984**, *106*, 4472.
(4) Calderwood, T. S.; Lee, W. A.; Bruice, T. C. *J. Am. Chem. Soc.* **1985**, *107*, 8272.
(5) Schappacher, M.; Weiss, R.; Montiel-Montoya, R.; Trautwein, A.; Tabard, A. *J. Am. Chem. Soc.* **1985**, *107*, 3736.
(6) Groves, J. T.; Quinn, R.; McMurry, T. J.; Nakamura, M.; Lang, G.; Boso, B. *J. Am. Chem. Soc.* **1985**, *107*, 354.
(7) Groves, J. T.; Gilbert, J. A. *Inorg. Chem.* **1986**, *25*, 123.
(8) Calderwood, T. S.; Bruice, T. C. *Inorg. Chem.* **1986**, *25*, 3722.
(9) Balch, A. L.; Renner, M. W. *J. Am. Chem. Soc.* **1986**, *108*, 2603.
(10) Swistak, C.; Mu, X. H.; Kadish, K. M. *Inorg. Chem.* **1987**, *26*, 4360.
(11) Gold, A.; Jayaraj, K.; Doppelt, P.; Weiss, R.; Chottard, G.; Bill, E.; Ding, X.; Trautwein, A. X. *J. Am. Chem. Soc.* **1988**, *110*, 5756.
(12) Shedbalkar, V. P.; Modi, S.; Mitra, S. *J. Chem. Soc., Chem. Commun.* **1988**, 1238.
(13) Balasubramanian, P. N.; Lindsay Smith, J. R.; Davies, M. J.; Kaaret, T. W.; Bruice, T. C. *J. Am. Chem. Soc.* **1989**, *111*, 1477.
(14) Chen, S.-M.; Su, Y. O. *J. Chem. Soc., Chem. Commun.* **1990**, 491.
(15) Arasasingham, R. D.; Balch, A. L.; Hart, R. L.; Latos-Grazynski, L. *J. Am. Chem. Soc.* **1990**, *112*, 7566.
(16) Bruice, T. C. *Acc. Chem. Res.* **1991**, *24*, 243.
(17) (a) Kadish, K. M.; Van Caemelbecke, E.; D'Souza, F.; Medforth, C. J.; Smith, K. M.; Tabard, A.; Guilard, R. *Organometallics* **1993**, *12*, 2411. (b) Kadish, K. M.; Van Caemelbecke, E.; D'Souza, F.; Medforth, C. J.; Smith, K. M.; Tabard, A.; Guilard, R. *Inorg. Chem.* **1995**, *34*, 2984.
(18) Jones, D. H.; Hinman, A. S.; Ziegler, T. *Inorg. Chem.* **1993**, *32*, 2092.
(19) Groves, J. T.; Gross, Z.; Stern, M. K. *Inorg. Chem.* **1994**, *33*, 5065.
(20) Rodgers, K. R.; Reed, R. A.; Su, Y. O.; Spiro, T. G. *Inorg. Chem.* **1992**, *31*, 2688.
(21) Kadish, K. M. *Prog. Inorg. Chem.* **1986**, *34*, 435.
(22) Kadish, K. M.; D'Souza, F.; Van Caemelbecke, E.; Boulas, P.; Vogel, E.; Aukauloo, A. M.; Guilard, R. *Inorg. Chem.* **1994**, *33*, 4474.
(23) (a) Collins, T. J.; Kostka, K. L.; Münck, E.; Uffelman, E. S. *J. Am. Chem. Soc.* **1990**, *112*, 5637. (b) Kostka, K. L.; Fox, B. G.; Hendrich, M. P.; Collins, T. J.; Rickard, C. E. F.; Wright, L. J.; Münck, E. *J. Am. Chem. Soc.* **1993**, *115*, 6746. (c) Collins, T. J. *Acc. Chem. Res.* **1994**, *27*, 279.
(24) Chen, S.-M.; Su, P.-J.; Su, Y. O. *J. Electroanal. Chem. Interfacial Electrochem.* **1990**, *294*, 361.

0020-1669/96/1335-0184$12.00/0

of octaethylcorrole, now provides the first examples of monomeric air-stable tetrapyrrole iron(IV) complexes.[25]

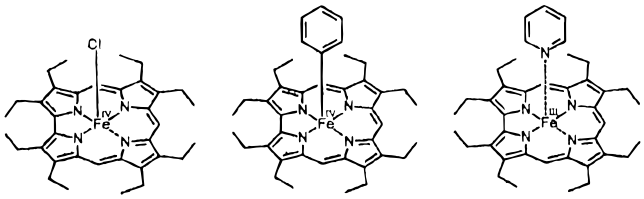

$(OEC)Fe^{IV}Cl$ $(OEC)Fe^{IV}(C_6H_5)$ $(OEC)Fe^{III}(py)$

Only a single iron corrole, (OEC)Fe(NO), has to date been electrochemically characterized.[26] This iron(III) nitrosyl derivative undergoes a total of five redox processes in benzonitrile containing 0.1 M tetra-*n*-butylammonium perchlorate (TBAP). The first reduction involves a conversion of Fe(III) to Fe(II), but the compound is apparently not oxidized to its iron(IV) form under the investigated solution conditions. It was therefore of interest to determine whether $(OEC)Fe^{IV}Cl$ and $(OEC)Fe^{IV}(C_6H_5)$ could both be electroreduced to their Fe(III) and Fe(II) forms or if other iron(III) corroles, such as (OEC)Fe(py), could be oxidized or reduced at the metal center to give Fe(IV) and Fe(II) derivatives, respectively. This question is now answered in the present paper, which reports the electrochemistry and spectroelectrochemistry of (OEC)FeCl, $(OEC)Fe(C_6H_5)$, and (OEC)Fe(py) in nonaqueous solvents containing either TBAP or tetra-*n*-ethylammonium hexafluorophosphate ($(TEA)PF_6$) as supporting electrolyte.

It has been suggested that the trianionic corrole macrocycle stabilizes metal ions in higher oxidation states than the dianionic porphyrin macrocycle,[25−27] and the presently investigated compounds may thus provide good model systems for studying synthetic high-valent iron complexes similar to those which have been shown to play a significant role in the reactivity of several enzymes.[28−32] The σ-bonded $(OEC)Fe(C_6H_5)$ derivative is of special interest since it is the first air-stable σ-bonded iron(IV) tetrapyrrole to be structurally characterized.[25] As will be shown in this paper, $(OEC)Fe(C_6H_5)$ undergoes two reversible oxidations, the first of which generates a stable iron(IV) π cation radical at room temperature.

To date, no spectroscopic characterizations of chemically or electrochemically generated phenyl σ-bonded iron(IV) tetrapyrrole π cation radicals or dications have appeared in the literature. This is in large part due to the fact that these derivatives, while formed on the cyclic voltammetry time scale,[3,18] also undergo a rapid migration of the phenyl group from the metal center to one of the four nitrogens of the porphyrin ring. This migration does not occur for neutral $(OEC)Fe(C_6H_5)$ in solution,[25] nor does it occur for the singly or doubly oxidized σ-bonded complexes, as will be shown in this present paper.

Experimental Section

Chemicals. The three investigated iron corroles, $(OEC)Fe(C_6H_5)$, (OEC)FeCl, and (OEC)Fe(py), were synthesized according to literature procedures.[25] Benzonitrile (PhCN) was purchased from Aldrich Chemical Co. and distilled over P_2O_5 under vacuum prior to use. Absolute dichloromethane (CH_2Cl_2) was dried over molecular sieves (4 Å), stored under argon, and distilled over CaH_2 prior to use. Anhydrous pyridine (99.8%), from Aldrich Chemical Co., was used without further purification. $CDCl_3$, used for NMR measurements, was obtained from Aldrich Chemical Co. and used as received. Tetra-*n*-butylammonium perchlorate was purchased from Sigma Chemical Co., recrystallized from ethyl alcohol, and dried under vacuum at 40 °C for at least 1 week prior to use. Tetra-*n*-ethylammonium hexafluorophosphate (electrochemical grade), from Fluka, was used as received. Silver perchlorate (99.9%), $AgClO_4 \cdot H_2O$, packed under argon, was purchased from Johnson Matthey Electronics and used as received.

Instrumentation. Cyclic voltammetry was carried out with an EG&G Model 173 potentiostat, an IBM Model EC 225 voltammetric analyzer, or a computerized multipurpose electrochemical device DACFAMOV (Microtec-CNRS-Toulouse, France) connected to an Apple II microcomputer, the latter of which was also used for rotating disk electrode (RDE) voltammetric experiments. A three-electrode system was used and consisted of a glassy carbon or platinum disk working electrode, a platinum wire counter electrode, and either a saturated calomel electrode (SCE) as the reference electrode or an Ag wire as the pseudo reference electrode. The SCE was separated from the bulk of the solution by a fritted-glass bridge of low porosity which contained the solvent/supporting electrolyte mixture. Ferrocene was used as an internal standard, but all potentials are referenced to the SCE.

^1H NMR spectra were recorded at 300 MHz on a Bruker AP 300 NMR spectrometer at 298 K. The solvent signal at $\delta = 7.24$ ppm was used as a standard. UV−visible spectra were recorded on a Perkin-Elmer Lambda 7 spectrophotometer, while IR measurements were performed with a Perkin-Elmer Series 1600. Mass spectra were carried out with a Finnigan H-SQ-30 using 3-nitrobenzyl alcohol as the matrix. Mössbauer spectra were obtained with a standard apparatus in the constant-acceleration mode containing a $^{57}Co/Rh$ source. Isomer shifts δ_{Fe} are referenced against α-Fe at room temperature. Magnetic susceptibility data were collected from 81 to 293 K with powdered samples using a Faraday balance. The data were corrected for diamagnetism (χ_{dia}) using a value of -300×10^{-6} cgsu.

UV−visible spectroelectrochemical experiments were carried out with a Hewlett Packard Model 8452A diode array spectrophotometer. The spectroelectrochemical cell was made from borosilicate glass and had an optical path length of *ca* 0.1 mm. The optically transparent thin layer electrode (OTTLE) used a platinum grid (1000 mesh).

ESR spectra were recorded on an IBM ER 100D spectrometer equipped with an ER 040-X microwave bridge and an ER 080 power supply or on a Bruker ESP 380E spectrometer. The *g* values were measured with respect to diphenylpicrylhydrazyl ($g = 2.0036 \pm 0.0003$).

Synthesis of $[(OEC)Fe(C_6H_5)]ClO_4$. A solution of 130 mg (0.2 mmol) of $(OEC)Fe(C_6H_5)$ in 10 mL of dichloromethane was stirred vigorously with 1 mL of a concentrated aqueous solution of iron(III) perchlorate for a period of 15 min as the color changed from red to brown. The organic layer was then washed thoroughly with 1 M perchloric acid, dried over sodium sulfate, and concentrated to a volume of 3 mL. After dropwise addition of 10 mL of *n*-pentane, the title compound precipitated as a fine brown powder. For purification, the oxidized iron corrole was digested by benzene and precipitated again from a dichloromethane solution using *n*-pentane (135 mg, 90%). *Caution!* Organic perchlorate salts can detonate spontaneously. Although no explosions were encountered in this work, precautions are warranted. The preparation of $[(OEC)Fe(C_6H_5)]ClO_4$ was always done on a small scale, and the material was not stored for long periods.

(25) Vogel, E.; Will, S.; Schulze Tilling, A.; Neumann, L.; Lex, J.; Bill, E.; Trautwein, A. X.; Wieghardt, K. *Angew. Chem., Int. Ed. Engl.* **1994**, *33*, 731.
(26) Autret, M.; Will, S.; Van Caemelbecke, E.; Lex, J.; Gisselbrecht, J.-P.; Gross, M.; Vogel, E.; Kadish, K. M. *J. Am. Chem. Soc.* **1994**, *116*, 9141.
(27) Adamian, V. A.; D'Souza, F.; Licoccia, S.; Di Vona, M. L.; Tassoni, E.; Paolesse, R.; Boschi, T.; Kadish, K. M. *Inorg. Chem.* **1995**, *34*, 532.
(28) Ator, M. A.; Ortiz de Montellano, P. R. in *The Enzymes*; Sigman, D. S., Boyer, P. D., Eds.; Academic Press: San Francisco, CA, 1990; Vol. XIX, p 214.
(29) Penner-Hahn, J. E.; Eble, K. S.; McMurry, T. J.; Renner, M.; Balch, A. L.; Groves, J. T.; Dawson, J. H.; Hodgson, K. O. *J. Am. Chem. Soc.* **1986**, *108*, 7819.
(30) Watanabe, Y.; Groves, J. T. In *The Enzymes*; Sigman, D. S., Boyer, P. D., Eds.; Academic Press: San Francisco, CA, 1990; Vol. XIX, p 406.
(31) McMurry, T. J.; Groves, J. T. In *Cytochrome P-450: Structure, Mechanism and Biochemistry;* Ortiz de Montellano, P. R., Ed.; Plenum Press : New York, 1986.
(32) Babcock, G. T.; Varotis, C. *J. Bioenerg. Biomemb.* **1993**, *25*, 71.

Table 1. Crystallographic Data for $[(OEC)Fe(C_6H_5)]ClO_4 \cdot 0.5C_2H_4Cl_2$

empirical formula	$C_{42}H_{50}Cl_2FeN_4O_4$
fw	801.64
space group	$P\bar{1}$
color, habit	black rhombus
crystal system	triclinic
radiation λ, Å	0.71069
μ(Mo Kα), mm^{-1}	0.497
T, K	293
d_{calcd}, g cm^{-3}	1.347
Z	2
a, Å	10.783(3)
b, Å	13.826(3)
c, Å	14.151(3)
α, deg	78.95(2)
β, deg	89.59(2)
γ, deg	72.98(2)
V, Å^3	1977.1(8)
data: unique/obsd	8603/8400
no. of parameters	670
R1 [F_o, $I_o > 2\sigma(I_o)$][a]	0.0864
wR2 (F_o^2)[b]	0.2293

[a] R1 = $[\sum||F_o| - |F_c||]/[\sum|F_o|]$. [b] wR2 = $\{[\sum w(F_o^2 - F_c^2)^2]/[\sum w(F_o^2)^2]\}^{1/2}$.

^{1}H NMR (300 MHz, $CDCl_3$): δ (ppm) = 23 (br singlet, 2H; CH_2), 21 (br singlet, 2H; CH_2), 17 (br singlet, 3H; H-5,15, H-10), 11.6 (br singlet, 2H; CH_2), 9.2 (br singlet, 2H; CH_2), 6.4 (br singlet, 2H; CH_2), 2.6 (br singlet, 2H; CH_2), 1.22 (br singlet, 6H; CH_3), 1.06 (br singlet, 6H; CH_3), 0.25 (br singlet, 6H; CH_3), 0.14 (br singlet, 6H; CH_3), −1.3 (br singlet, 2H; CH_2), −10.0 (br singlet, 2H; CH_2); resonances of the axial ligand were not detected due to line broadening. MS (FAB, 3-NBA), *m/z* (relative intensity): 652 (84) $[(OEC)Fe(C_6H_5)]^{\bullet+}$, 575 (100) $[(OEC)Fe]^+$, 560 (30) $[(OEC)Fe\text{-}CH_3^{\bullet}]^{\bullet+}$, 545 (45) $[(OEC)Fe - 2CH_3^{\bullet}]^+$. IR (CsI), ν (cm^{-1}): 2965, 2930, 2870, 1551, 1504, 1469, 1448, 1374, 1315, 1270, 1103 ($\nu(ClO_4^-)$), 1085 ($\nu(ClO_4^-)$), 1055, 1013, 985, 957, 877, 831, 727, 625 ($\nu(ClO_4^-)$). UV−vis (CH_2Cl_2), λ_{max} (nm) (ϵ, M^{-1} cm^{-1}): 341 (48 900) sh, 365 (56 000), 424 (12 300) sh, 455 (9600) sh, 516 (5400) sh, 612 (2400) sh. Mössbauer parameters (120 K): $\delta_{Fe} = -0.10$ mm s^{-1}, $\Delta E_q = 3.66$ mm s^{-1}. Magnetic moment: $\mu_{eff} = 1.78\ \mu_B$ (293 K); $\mu_{eff} = 1.62\ \mu_B$ (81 K). Anal. Calcd for $C_{41}H_{48}N_4FeClO_4$: C, 65.47; H, 6.43; N, 7.45; Cl, 4.71. Found: C, 65.22; H, 6.39; N, 7.40; Cl, 4.37.

X-ray Structural Determination of $[(OEC)Fe(C_6H_5)]ClO_4$. Single crystals of $[(OEC)Fe(C_6H_5)]ClO_4 \cdot 0.5C_2H_4Cl_2$ were grown by slow diffusion of *n*-pentane into a concentrated solution of $[(OEC)Fe(C_6H_5)]ClO_4$ in dichloroethane. X-ray data were collected on an Enraf-Nonius CAD4 diffractometer using monochromated Mo Kα radiation. Experimental conditions are given in Table 1. Cell parameters were determined by least-squares refinement of 25 arbitrary reflections. The intensities of two standard reflections were checked during data collection every 2 h. The structure was solved by direct methods (Mo1EN) and refined for all observed reflections (non-hydrogen atoms with anisotropic and hydrogen atoms with isotropic temperature factors) using the SHELXL-93 program package.[26] The occupancy factor of the dichloroethane molecule (which exhibits an inversion center) was chosen as 1. Hydrogen atoms of the ethyl substituents were refined with idealized parameters (C−H = 0.96 Å, H−C−H = 109.5°). The final model shows no electron peaks and holes larger than 0.895 and −0.905 e/Å^3, respectively.

Results and Discussion

Electrochemistry of $(OEC)Fe^{IV}(C_6H_5)$. The σ-bonded complex undergoes two reductions and three oxidations in PhCN, 0.1 M TBAP (see Figure 1a and Table 2). The two reductions, at $E_{1/2} = -0.61$ and −1.98 V (processes I and II), and first two oxidations, at $E_{1/2} = 0.47$ and 1.20 V (processes III and IV), are all reversible and involve the addition or abstraction of a single electron. In contrast, the third oxidation (process V) is irreversible due to a chemical reaction following electron transfer and occurs at $E_p = +1.73$ V for a scan rate of 0.1 V/s. Processes I, III, and IV are also reversible in CH_2Cl_2, 0.1 M (TEA)PF_6 and occur at similar half-wave potentials as in PhCN containing 0.1 M TBAP ($E_{1/2}$ = -0.62, 0.43, and 1.26 V). However, processes II and V were not detected in CH_2Cl_2 due to the smaller potential window of this solvent as compared to PhCN.

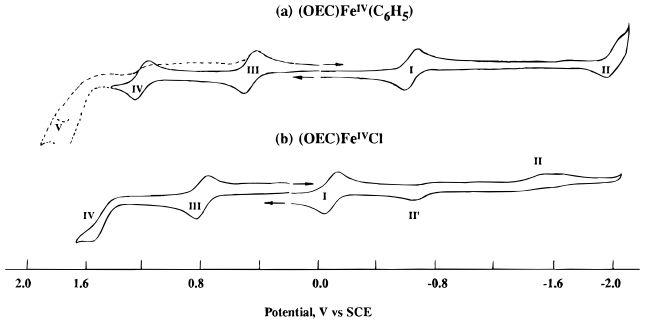

Figure 1. Cyclic voltammograms of (a) $(OEC)Fe(C_6H_5)$ and (b) (OEC)FeCl, in PhCN containing 0.1 M TBAP. Scan rate = 0.1 V/s.

Table 2. Half-Wave Potentials (V vs SCE) for Reduction and Oxidation of the Iron Corroles

		oxidation			reduction	
compound	solvent[a]	3rd	2nd	1st	1st	2nd
$(OEC)Fe(C_6H_5)$	PhCN	+1.73[b]	+1.20	+0.47	−0.61	−1.98
	CH_2Cl_2		+1.26	+0.43	−0.62	
(OEC)FeCl	PhCN		+1.50[b]	+0.79	−0.07	−1.45[b]
	CH_2Cl_2		+1.44[d]	+0.76	−0.08	
$(OEC)FeClO_4$[c]	PhCN			+0.25	−0.68	
(OEC)Fe(py)	CH_2Cl_2		+1.03	+0.21	−1.04[b]	
	py			+0.28	−0.94	

[a] The supporting electrolyte was 0.1 M TBAP for PhCN and pyridine and 0.1 M (TEA)PF_6 for CH_2Cl_2. [b] Irreversible process; value given is peak potential at a scan rate of 0.1 V/s. [c] *In-situ*-generated by addition of $AgClO_4 \cdot H_2O$ to (OEC)FeCl (see text). [d] Value obtained in CH_2Cl_2, 0.1 M TBAP at −50 °C.

Electrochemistry of (OEC)FeCl. The first oxidation and first reduction of this formal iron(IV) complex involve one-electron transfers in CH_2Cl_2, 0.1 M (TEA)PF_6 and occur at $E_{1/2}$ = +0.76 and −0.08 V, as seen by both cyclic and RDE voltammetry. Again, a larger number of electrode reactions are observed in PhCN, 0.1 M TBAP, where two oxidations and two reductions can be detected (see Figure 1b and Table 2). The first oxidation is reversible and occurs at $E_{1/2} = +0.79$ V. The second is irreversible at room temperature ($E_{pa} = 1.50$ V for a scan rate of 0.1 V/s) but becomes reversible when the temperature of the solution is lowered to 0 °C and/or when the potential scan rate is increased to 0.3 V/s or above. The first reduction of (OEC)FeCl (process I) is also reversible ($E_{1/2}$ = −0.07 V), but the second (process II) is drawn out, occurs at $E_{pc} = -1.45$ V for a scan rate of 0.1 V/s, and is coupled to a well-defined reoxidation peak (process II′) at $E_{pa} = -0.62$ V.

Process II is proposed to involve the reduction of $[(OEC)Fe^{III}Cl]^-$ to $[(OEC)Fe^{II}]^-$ at $E_{pc} = -1.45$ V while process II′ is proposed to involve the reoxidation of $[(OEC)Fe^{II}]^-$, which is formed after dissociation of Cl^- from the doubly reduced corrole. The electrogenerated $[(OEC)Fe^{III}Cl]^-$ species also exists in equilibrium with $(OEC)Fe^{III}$, as shown in eq 1, and this results in the small cathodic peak at −0.80 V due to a reduction of the unligated species.

$$[(OEC)FeCl]^- \rightleftarrows (OEC)Fe + Cl^- \quad (1)$$

The occurrence of the above equilibrium was confirmed by recording cyclic voltammograms after the *in-situ* addition of 1

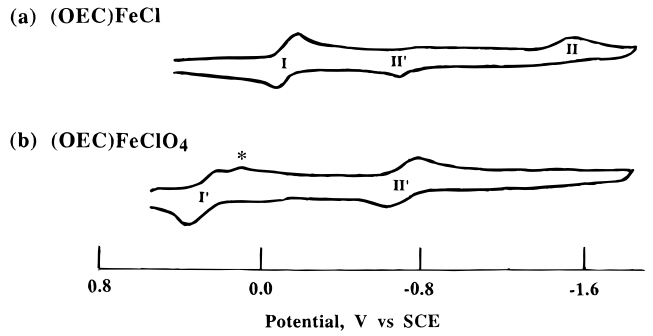

Figure 2. Cyclic voltammograms of (a) (OEC)FeCl and (b) (OEC)-$FeClO_4$ in PhCN, 0.1 M TBAP. The latter compound was *in situ* generated by addition of 1 equiv of $AgClO_4 \cdot H_2O$ to (OEC)FeCl in PhCN. The star (*) represents the reduction of adsorbed Ag^+.

Scheme 1

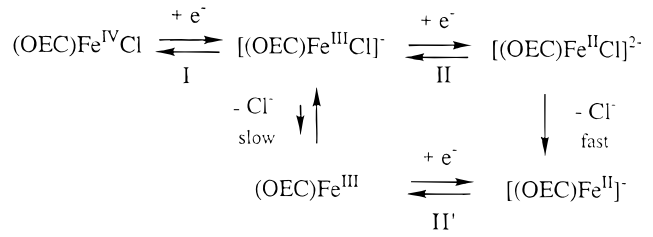

equiv of $AgClO_4 \cdot H_2O$ to (OEC)FeCl in PhCN, which leads to the formation of $(OEC)FeClO_4$, as shown in eq 2.

$$(OEC)FeCl + AgClO_4 \rightarrow (OEC)FeClO_4 + AgCl \quad (2)$$

The *in-situ*-generated $(OEC)FeClO_4$ undergoes reversible one-electron reductions at $E_{1/2} = +0.25$ and -0.68 V (Figure 2). These two reductions are assigned to the stepwise conversion of $(OEC)Fe^{IV}ClO_4$ to $(OEC)Fe^{III}$ (reaction I′) and then $(OEC)Fe^{III}$ to $[(OEC)Fe^{II}]^-$ (reaction II′) as shown in eq 3. The

$$(OEC)FeClO_4 \overset{I'}{\rightleftharpoons} (OEC)Fe \overset{II'}{\rightleftharpoons} [(OEC)Fe]^- \quad (3)$$

anodic peak for process II′ in Figure 2b is located at a potential similar to E_{pa} for process II′ of (OEC)FeCl in Figure 2a, thus giving further evidence that the same species are involved in both electrode reactions, *i.e.*, $(OEC)Fe^{III}$ and $[(OEC)Fe^{II}]^-$.

Attempts were made to obtain a reversible process II in Figure 2a by the addition of excess Cl^- to solutions of (OEC)FeCl in PhCN, but this was unsuccessful, which indicates a rapid dissociation of the Cl^- ligand after electrogeneration of $[(OEC)Fe^{II}Cl]^{2-}$. Thus, the complete set of reactions which occur during the reduction and reoxidation of (OEC)FeCl in PhCN can be represented as shown in Scheme 1.

In summary, two different forms of the iron(III) corroles exist in solution after the first one-electron reduction of (OEC)FeCl at -0.08 V. One is $[(OEC)FeCl]^-$, which is anionic, and the other is (OEC)Fe, which is neutral (see Scheme 1). The equilibrium between these two singly reduced complexes favors $[(OEC)FeCl]^-$ over (OEC)Fe, as indicated by the fact that the cathodic reduction currents of process II′ are much smaller than those of process II, despite the 750 mV difference in potentials which should thermodynamically favor an electroreduction of (OEC)Fe over the more difficult to reduce $[(OEC)FeCl]^-$.[33]

(33) (a) Large differences in potential are also seen between unligated and ligated porphyrins of the types (P)FeCl and $[(P)Fe]^+$ where P = OEP ($\Delta E_{1/2} = 520$ mV)[33b] or TPP ($\Delta E_{1/2} = 490$ mV).[21] (b) Kadish, K. M.; Bottomley, L. A.; Kelly, S.; Schaeper, D.; Shiue, L. R. *Bioelectrochem. Bioenerg.* **1981**, *8*, 213.

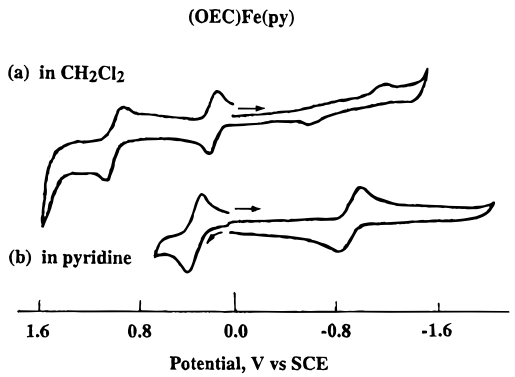

Figure 3. Cyclic voltammograms of (OEC)Fe(py) in (a) CH_2Cl_2, 0.1 M $(TEA)PF_6$ and (b) pyridine, 0.1 M TBAP.

Scheme 2

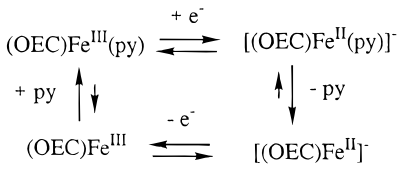

Electrochemistry and Spectroelectrochemistry of (OEC)-Fe(py). (OEC)Fe(py) undergoes reversible one-electron oxidations at $E_{1/2} = +0.21$ and $+1.03$ V in CH_2Cl_2, 0.1 M $(TEA)PF_6$ (see Figure 3a and Table 2). An irreversible reduction is also observed at $E_{pc} = -1.04$ V (scan rate 0.1 V/s), and this process is coupled to a reoxidation peak at $E_{pa} = -0.60$ V. The latter potential is similar to the $E_{1/2}$ for oxidation of $[(OEC)Fe]^-$ (Figure 2b), which suggests a fast dissociation of the pyridine axial ligand upon the first reduction of (OEC)Fe(py) in CH_2Cl_2. The resulting $[(OEC)Fe]^-$ product is then reoxidized to (OEC)Fe at -0.60 V, after which a pyridine molecule reassociates as illustrated by the overall mechanism shown in Scheme 2.

The first reduction of (OEC)Fe(py) in pyridine, 0.2 M TBAP occurs at $E_{1/2} = -0.94$ V and is reversible to quasireversible (see Figure 3b). The electrochemical data suggest that the bound pyridine axial ligand on (OEC)Fe(py) remains coordinated after reduction in neat pyridine on the cyclic voltammetry time scale.

Spectral Monitoring of the Fe(III)/Fe(IV) Processes. The UV−visible changes observed during the first one-electron reduction of $(OEC)Fe^{IV}(C_6H_5)$ and $(OEC)Fe^{IV}Cl$ in CH_2Cl_2 are shown in Figure 4a,b and these spectra can be compared to the changes seen upon the conversion of $(OEC)Fe^{III}(py)$ to its singly oxidized product (Figure 4c). The neutral Fe(IV) forms of $(OEC)Fe(C_6H_5)$ and (OEC)FeCl (shown by solid lines) are characterized by Soret bands at 380 and 372 nm, respectively, while singly oxidized (OEC)Fe(py), which also contains Fe(IV) and is shown by a solid line in Figure 4c, has a single band at 381 nm (see Table 3). The two singly reduced, Fe(III), compounds (illustrated by dashed lines) have similar bands which are located at 404 and 534 nm for $[(OEC)Fe(C_6H_5)]^-$ and at 398 and 536 nm for $[(OEC)FeCl]^-$. These data can be compared to those for neutral $(OEC)Fe^{III}(py)$ (dashed line in Figure 4c), which has bands at 398 and 547 nm (see Table 3). Several isosbestic points are seen in Figure 4a−c, thus indicating the lack of spectral intermediates upon the conversion of Fe-(IV) to Fe(III) or vice versa.

The one-electron reduction of $(OEC)Fe(C_6H_5)$ in THF or PhCN leads to an EPR spectrum of the type shown in Figure 5a. The spectrum is rhombic with $g_z = 2.51$, $g_y = 2.19$, and $g_x = 1.93$. It is similar to the EPR spectra of several d^5 low-spin

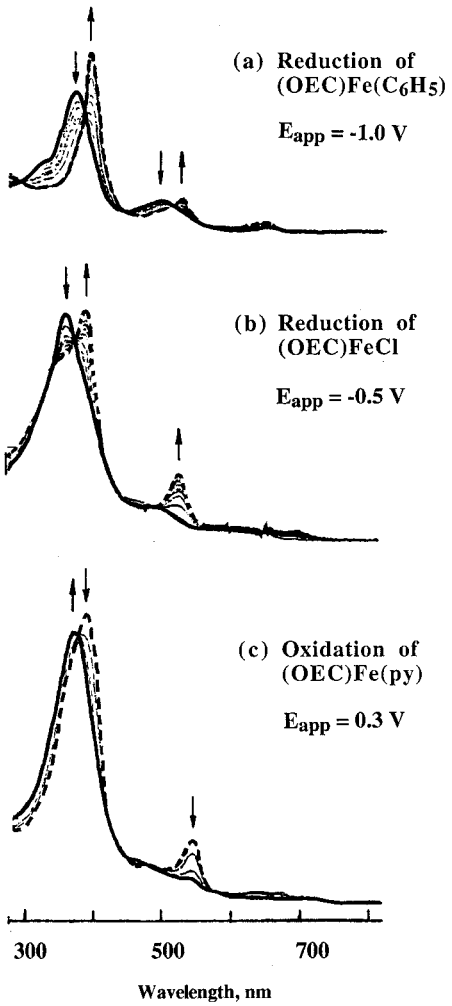

Figure 4. Thin-layer spectral changes obtained upon controlled-potential reduction in CH_2Cl_2, 0.2 M (TEA)PF_6 of (a) (OEC)Fe(C_6H_5) and (b) (OEC)FeCl and (c) upon oxidation of (OEC)Fe(py) in pyridine, 0.2 M TBAP. The Fe(IV) forms of each compound are given by solid lines (—) while the Fe(III) forms are given by dashed lines (---).

iron(III) porphyrins.[34−38] It also has a shape similar to that of the σ-bonded (OEP)Fe^{III}(C_6H_4-*p*-OCH_3) complex which has *g* values at 2.023, 2.001, and 1.982.[36] The EPR spectrum obtained after the one-electron reduction of (OEC)Fe^{IV}Cl in PhCN (Figure 5b) shows a signal with $g_\perp \approx 4.9$ and $g_\parallel \approx 2.0$, indicative of an intermediate-spin ($S = {}^3/_2$) iron(III) corrole.[34] All attempts to isolate [(OEC)Fe^{III}(C_6H_5)]$^-$ by chemical reduction of (OEC)-Fe^{IV}(C_6H_5) failed.

(OEC)Fe(py) was characterized by susceptibility measurements as containing an intermediate-spin $S = {}^3/_2$ iron(III) metal center in the solid state,[25] and a similar spin state assignment can be made in CH_2Cl_2 or PhCN at 77 K, where EPR spectra show the characteristic[34] $S = {}^3/_2$ signals at $g_\perp \approx 4.5$ and $g_\parallel \approx 2.0$ (see Figure 5c for PhCN data). The EPR spectrum of (OEC)Fe(py) is more complicated in neat pyridine at 77 K and shows not only absorptions at $g_\perp \approx 4.5$ and $g_\parallel \approx 2.0$ but also a rhombic signal with $g_z = 2.5$, $g_y = 2.2$, and $g_x = 1.8$ (Figure 5c). This result is consistent with an earlier suggestion that two forms of the Fe(III) corrole might be present in pyridine.[52] One contains a low-spin ($S = {}^1/_2$) iron(III) and is characterized by a rhombic signal, while the other contains an intermediate-spin ($S = {}^3/_2$) iron(III) and is characterized by $g_\perp \approx 4.5$ and $g_\parallel \approx 2.0$. We suggest that the $S = {}^3/_2$ signal in pyridine at 77 K belongs to the initial (OEC)Fe(py) complex, while the $S = {}^1/_2$ signal belongs to (OEC)Fe$(py)_2$, a compound which is formed in neat pyridine solutions at low temperature.

Spectral Characterization of Fe(IV) π Cation Radicals. The one-electron oxidation of (OEC)Fe(C_6H_5) and (OEC)FeCl leads to [(OEC)Fe(C_6H_5)]$^+$ and [(OEC)FeCl]$^+$, compounds which may be described by three formulations depending upon the site of electron transfer (*i.e.* oxidation of the central metal ion or oxidation of the macrocycle): (i) an Fe(V) corrole with an unoxidized π ring system, (ii) an Fe(IV) corrole π cation radical, and (iii) an Fe(III) corrole dication. To evaluate the site of electron transfer and to confirm an exact formulation, we have performed UV−visible and EPR measurements on each of the singly oxidized derivatives. The stability of singly oxidized [(OEC)Fe(C_6H_5)]$^+$ also allows for isolation of the cation in a substantial amount, making Mössbauer and susceptibilty measurements accessible. For this purpose, (OEC)Fe^{IV}-(C_6H_5) was oxidized with iron(III) perchlorate (see Experimental Section), yielding [(OEC)Fe(C_6H_5)]ClO_4, which was easily crystallized.

The Mössbauer spectrum of [(OEC)Fe(C_6H_5)]ClO_4 at 120 K consists of a symmetrical quadrupole doublet with an isomer shift $\delta_{Fe} = -0.10$ mm/s and a quadrupole splitting $\Delta E_q = 3.66$ mm/s. These parameters are virtually identical to those of (OEC)Fe(C_6H_5) ($\delta_{Fe} = -0.11$ mm/s and $\Delta E_q = 3.72$ mm/s)[25] (see Figure 6), suggesting the presence of an iron(IV) center before and after oxidation of (OEC)Fe(C_6H_5). The Mössbauer data rules out the formulation of the singly oxidized compound as an iron(V) corrole or as an iron(III) corrole dication but are consistent with generation of an iron(IV) corrole π cation radical upon the first one-electron oxidation of (OEC)Fe^{IV}(C_6H_5).

The above assignment is also implied by the UV−visible spectral changes upon oxidation. These are shown in Figure 7 and differ significantly from those seen in Figure 4, where only metal-centered reactions occur. The UV−visible spectra of [(OEC)Fe(C_6H_5)]$^+$ and [(OEC)FeCl]$^+$ both have a split Soret band (see Table 4), while the spectra of their neutral iron(IV) counterparts have only a single Soret band in each case (see Table 3).

The formulation of [(OEC)Fe(C_6H_5)]$^+$ and [(OEC)FeCl]$^+$ as Fe(IV) corrole π cation radicals leads formally to compounds having three unpaired electrons, two on the d^4 iron(IV) and the third on the corrole macrocycle. These electrons can interact in an antiferromagnetic or ferromagnetic manner leading to an $S = {}^1/_2$ or $S = {}^3/_2$ ground state, respectively. The magnetic susceptibility data for solid [(OEC)Fe(C_6H_5)]ClO_4 were obtained by the Faraday method from 81 to 293 K. These measurements show that the complex exhibits a well-separated $S = {}^1/_2$ ground state, because a nearly temperature-independent magnetic moment is observed ($\mu_{eff} = 1.78\ \mu_B$ at 293 K). Thus a strong antiferromagnetic coupling between the unpaired electron of the corrole π ring system ($S_R = {}^1/_2$) and the electrons of the metal center ($S_M = 1$) occurs, resulting in a compound where the unpaired electron formally remains on the central iron.

Evidence for this coupling scheme is also given by the rhombic EPR spectra of [(OEC)Fe(C_6H_5)]$^+$ and [(OEC)FeCl]$^+$, which are shown in Figure 8. These spectra are characteristic of an $S = {}^1/_2$ system and are similar in shape to those of the corresponding Fe(III) derivatives in Figure 5. The *g* values (see

(34) Palmer, G. In *Iron Porphyrins. Part Two;* Lever, A. B. P., Gray, H. B., Eds.; Addison-Wesley: Reading, MA, 1983; p 43.
(35) Taylor, C. P. S. *Biochim. Biophys. Acta* **1977**, *491*, 137.
(36) Ogoshi, H.; Sugimoto, H.; Yoshida, Z.-I.; Kobayashi, H.; Sakai, H.; Maeda, Y. *J. Organomet. Chem.* **1982**, *234*, 185.
(37) Walker, F. A.; Huynh, B. H.; Scheidt, W. R.; Osvath, S. R. *J. Am. Chem. Soc.* **1986**, *108*, 5288.
(38) Safo, M. K.; Walker, F. A.; Raitsimring, A. M.; Walters, W. P.; Dolata, D. P.; Debrunner, P. G.; Scheidt, W. R. *J. Am. Chem. Soc.* **1994**, *116*, 7760.

Table 3. UV−Visible Data (λ, nm)[a] for Iron(IV) and Iron(III) Corroles

initial compd	reacn[b]	Fe(IV) species		reacn[b]	Fe(III) species		
$(OEC)Fe^{IV}(C_6H_5)$	none	380 (66.1)	508 (14.9)	1st redn	404 (85.8)	534 (14.9)	658 (3.7)
$(OEC)Fe^{IV}Cl$	none	372 (57.4)		1st red	398 (50.7)	536 (13.3)	
$(OEC)Fe^{III}(py)$[c]	1st oxidn	381 (71.7)		none	398 (67.2)	547 (15.2)	

[a] Data are given in CH_2Cl_2, and values in parentheses are $10^{-3}\epsilon$ in L/(mol cm). [b] See Table 2 for $E_{1/2}$ of first oxidation or first reduction. [c] Values are given in pyridine.

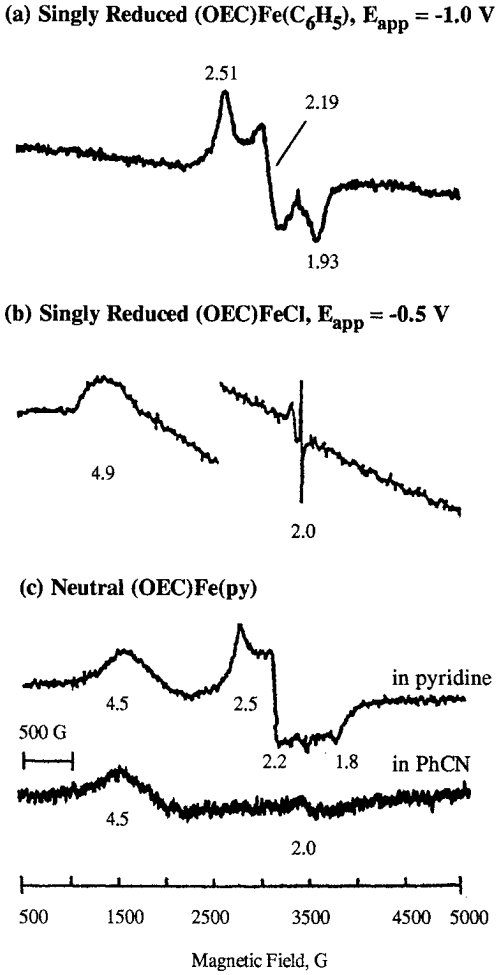

Figure 5. EPR spectra of (a) singly reduced $(OEC)Fe(C_6H_5)$ in THF at 120 K, (b) singly reduced (OEC)FeCl in PhCN at 77 K, and (c) neutral (OEC)Fe(py) in pyridine and PhCN at 77 K. The g values are given in the figure.

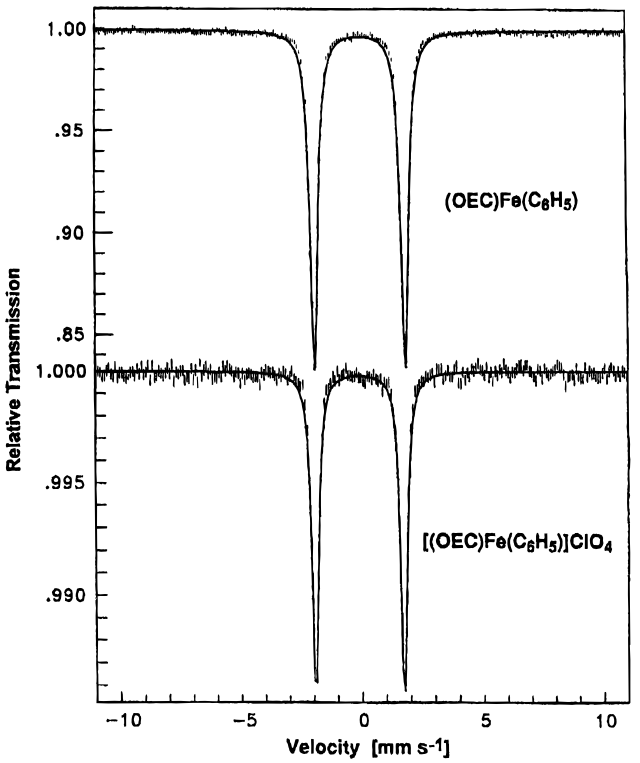

Figure 6. Mössbauer spectra of polycrystalline $(OEC)Fe(C_6H_5)$ (top, 77 K) and its oxidation product $[(OEC)Fe(C_6H_5)]ClO_4$ (bottom, 120 K) at zero field.

Table 4) are equal to 2.17, 2.04, and 2.01 for $[(OEC)Fe(C_6H_5)]^+$ and 2.12, 2.07, and 2.02 for $[(OEC)FeCl]^+$, indicating an $S = {}^1/_2$ ground state for both complexes. Both EPR spectra rule out formation of an Fe(V) oxidation product, since the expected d^3 high-spin ($S = {}^3/_2$) Fe(V) would have a signal at $g \approx 4$, similar to what was observed for oxoiron(V) porphyrins.[39] This is not the case, and neither $[(OEC)Fe(C_6H_5)]^+$ nor $[(OEC)FeCl]^+$ shows signals around $g \approx 4$.

It is perhaps of interest to point out that the EPR spectra of (oxoferryl)porphyrin π cation radicals show a ferromagnetic coupling between the iron(IV) center and the porphyrin π cation radical; *i.e.*, the (oxoferryl)porphyrin π cation radicals behave as a $S = {}^3/_2$ system.[40,41] The strong antiferromagnetic spin−spin interaction also distinguishes the oxidized iron corrole from compound II of horseradish peroxidase, which exhibits only a weak ferromagnetic coupling.[45] Oxoferryl π cation radicals have been spectroscopically characterized, but these species are quite reactive and can only be stabilized at low temperature.[42,43] To our knowledge, only a single iron(IV) π cation radical has been shown to be stable at room temperature, and this compound was obtained upon the abstraction of two electrons from dimeric $[(TPP)Fe]_2N$.[44] The two iron(IV) corrole π cation radicals reported in this paper are therefore the first examples of such monomeric species which are stable at room temperature.

$[(OEC)Fe(C_6H_5)]^+$ was structurally characterized as a perchlorate salt (see Tables 1, 5, 6, and 7). The ORTEP diagram of the cation is shown in Figure 9. The unit cell is shown in

(39) Yamaguchi, K.; Watanabe, Y.; Morishima, I. *J. Chem. Soc., Chem. Commun.* **1992**, 1721.

(40) (a) Mandon, D.; Weiss, R.; Jayaraj, K.; Gold, A.; Terner, J.; Bill, E.; Trautwein, A. X. *Inorg. Chem.* **1992**, *31*, 4404. (b) Gold, A.; Jayaraj, K.; Doppelt, P.; Weiss, R.; Bill, E.; Ding, X.-Q.; Bominaar, E. L.; Trautwein, A. X.; Winkler, H. *New. J. Chem.* **1989**, *13*, 169.

(41) (a) Bill, E.; Ding, X.-Q.; Bominaar, E. L.; Trautwein, A. X.; Winkler, H.; Mandon, D.; Weiss, R.; Gold, A.; Jayaraj, K.; Hatfield, W. E.; Kirk, M. L. *Eur. J. Biochem.* **1990**, *188*, 665. (b) Ochsenbein, P.; Mandon, D.; Fischer, J.; Weiss, R.; Austin, R.; Jayaraj, K.; Gold, A.; Terner, J.; Bill, E.; Müther, M.; Trautwein, A. X. *Angew. Chem., Int. Ed. Engl.* **1993**, *32*, 1437.

(42) Groves, J. T.; Haushalter, R. C.; Nakamura, M.; Nemo, T. E.; Evans, B. J. *J. Am. Chem. Soc.* **1981**, *103*, 2884.

(43) Groves, J. T.; Watanabe, Y. *J. Am. Chem. Soc.* **1988**, *110*, 8443.

(44) English, D. R.; Hendrickson, D. N.; Suslick, K. S. *Inorg. Chem.* **1985**, *24*, 121.

(45) (a) Schultz, C. E.; Devaney, P. W.; Winkler, H.; Debrunner, P. G.; Doan, N.; Chiang, R.; Rutter, R.; Hager, L. P. *FEBS Lett.* **1979**, *103*, 102. (b) Roberts, J. E.; Hoffmann, B. M.; Rutter, R.; Hager, L. P. *J. Biol. Chem.* **1981**, *256*, 2118.

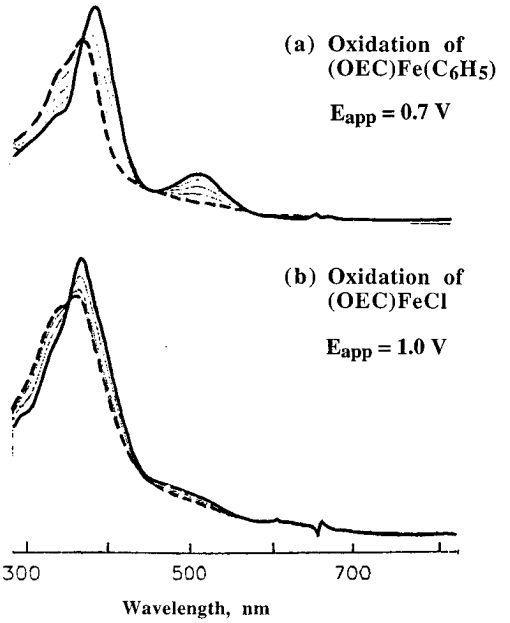

Figure 7. Thin-layer spectral changes obtained upon controlled-potential oxidation in CH_2Cl_2, 0.2 M (TEA)PF_6 of (a) (OEC)Fe(C_6H_5) and (b) (OEC)FeCl. The Fe(IV) forms of the compounds are given by solid lines (—) while the Fe(IV) π cation radicals are indicated by dashed lines (---).

Table 4. UV−Visible and EPR Spectral Data for Iron(IV) Corrole π Cation Radicals

	λ, nm ($10^{-3}\epsilon$, L/(mol cm))[a]		g values[b]		
$[(OEC)Fe^{IV}(C_6H_5)]^+$	342 (53.6)	366 (62.5)	2.17	2.04	2.01
$[(OEC)Fe^{IV}Cl]^+$	342 (45.4)	366 (48.0)	2.12	2.07	2.02

[a] In CH_2Cl_2. [b] In PhCN at 77 K.

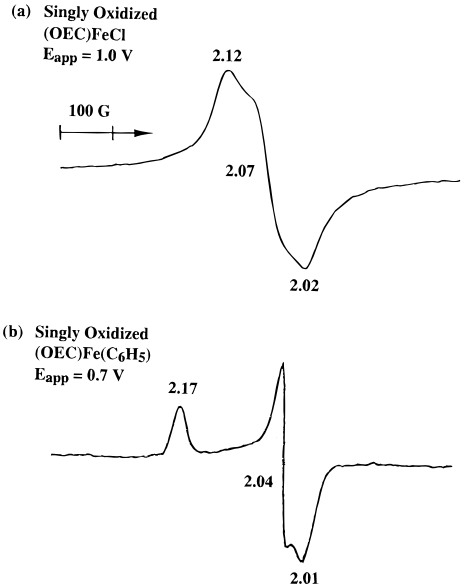

Figure 8. EPR spectra of electrogenerated (a) $[(OEC)FeCl]^+$ and (b) $[(OEC)Fe(C_6H_5)]^+$ at 77 K in PhCN. The g values are given in the figure.

Figure 10 and indicates that the iron corrole unit in [(OEC)-Fe(C_6H_5)]ClO_4·0.5$C_2H_4Cl_2$ forms a $\pi-\pi$ dimer with structural parameters similar to those of the neutral compound (see Table 5). The mean plane separation of the corrole ligands in the $\pi-\pi$ dimer of [(OEC)Fe(C_6H_5)]ClO_4 is 3.53 Å, which is distinctly larger than the 3.21 Å between the two π cation radicals of [(OEC)Fe(NO)]$FeCl_4$.[26] The iron atom in [(OEC)-Fe(C_6H_5)]ClO_4 is five-coordinated and exhibits bond lengths

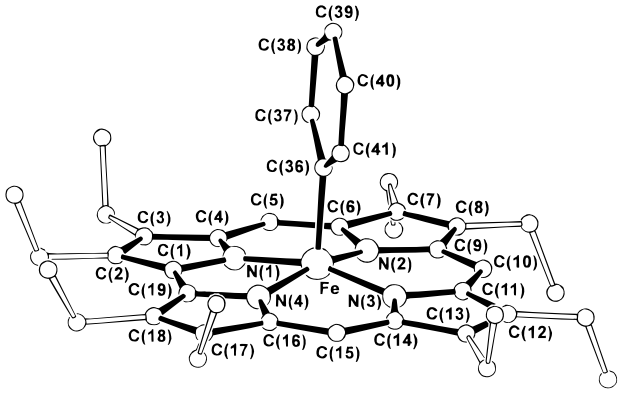

Figure 9. ORTEP diagram of the cation of [(OEC)Fe(C_6H_5)]-ClO_4·0.5$C_2H_4Cl_2$ (perspective view, hydrogen atoms omitted for clarity) displaying the atom-labeling scheme for the core atoms in Tables 6 and 7. Atoms are contoured with arbitrary size.

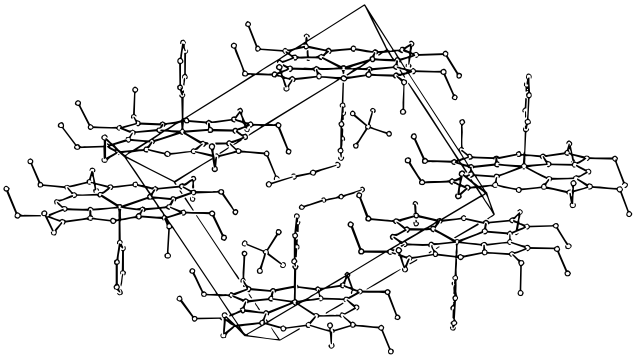

Figure 10. Unit cell of [(OEC)Fe(C_6H_5)]ClO_4·0.5$C_2H_4Cl_2$.

Table 5. Selected Bond Lengths and Distances (Å) for (OEC)Fe(C_6H_5) and [(OEC)Fe(C_6H_5)]ClO_4·0.5$C_2H_4Cl_2$

	(OEC)Fe(C_6H_5)	[(OEC)Fe(C_6H_5)]ClO_4·0.5$C_2H_4Cl_2$
Fe−N[a]	1.871(3)	1.864(3)
Fe−C_6H_5	1.984(3)	1.965(5)
ΔN_4[b]	0.272(1)	0.242(2)
Fe···Fe[c]	5.437	5.321
mps[d]	3.53	3.53
ls[e]	3.49	3.44

[a] Average values. [b] Displacement of the iron atom with respect to the mean plane of the four nitrogen atoms. [c] Intermolecular iron−iron distance. [d] Mean plane separation of the corrole ligands in the $\pi-\pi$ dimer. [e] Lateral shift of the corrole ligands in the $\pi-\pi$ dimer.

and distances which are slightly smaller than those in (OEC)-Fe(C_6H_5) (Table 5). Due to the small out-of-plane position of the iron, the corrole ligand in [(OEC)Fe(C_6H_5)]ClO_4 adopts a nearly planar conformation, and the maximum distance of a C,N atom from the mean plane of the 23-atom core is only 0.70 Å.

The oxidation of the corrole macrocycle leads to a characteristic bond length pattern in the inner 15-membered ring of the corrole macrocycle (see Table 6). For [(OEC)Fe(C_6H_5)]-ClO_4, a sequence of alternating longer and shorter bonds is established (mostly pronounced for the C−N bonds of the bipyrrolic substructure), a structural feature which is not observed for metallocorroles containing an intact corrole ligand.[25,26,46] This tendency for π-bond localization also occurs for some metalloporphyrins which are oxidized at the site of the ligand.[47] In the porphyrin series, this distortion could be confirmed by theoretical calculations.[48]

(46) Paolesse, R.; Licoccia, S.; Bandali, G.; Dolmella, A.; Boschi, T. *Inorg. Chem.* **1994**, *33*, 1171.

Table 6. Selected Bond Lengths (Å) for $[(OEC)Fe(C_6H_5)]ClO_4 \cdot 0.5C_2H_4Cl_2$[a]

Fe−N(1)	1.847(3)	C(3)−C(4)	1.450(5)
Fe−N(4)	1.853(3)	C(4)−C(5)	1.405(6)
Fe−N(3)	1.876(3)	C(5)−C(6)	1.384(6)
Fe−N(2)	1.879(3)	C(6)−C(7)	1.457(6)
Fe−C(36)	1.965(5)	C(7)−C(8)	1.354(7)
N(1)−C(4)	1.348(5)	C(8)−C(9)	1.461(5)
N(1)−C(1)	1.414(5)	C(9)−C(10)	1.379(6)
N(2)−C(9)	1.373(5)	C(10)−C(11)	1.396(6)
N(2)−C(6)	1.410(5)	C(l l)−C(12)	1.460(6)
N(3)−C(11)	1.370(5)	C(12)−C(13)	1.364(7)
N(3)−C(14)	1.404(5)	C(13)−C(14)	1.446(6)
N(4)−C(16)	1.349(5)	C(14)−C(15)	1.374(6)
N(4)−C(19)	1.407(5)	C(15)−C(16)	1.396(6)
C(1)−C(19)	1.386(5)	C(16)−C(17)	1.444(5)
C(1)−C(2)	1.434(5)	C(17)−C(18)	1.358(6)
C(2)−C(3)	1.376(6)	C(18)−C(19)	1.450(5)

[a] Only values for the corrole macrocycle are given. Numbers in parentheses are estimated standard deviations in the least significant digit.

Table 7. Selected Bond Angles (deg) for $[(OEC)Fe(C_6H_5)]ClO_4 \cdot 0.5C_2H_4Cl_2$[a]

N(1)−Fe−N(4)	80.40(14)	C(6)−C(5)−C(4)	123.3(4)
N(1)−Fe−N(3)	163.2(2)	C(5)−C(6)−N(2)	124.0(4)
N(4)−Fe−N(3)	90.93(14)	C(5)−C(6)−C(7)	127.5(4)
N(1)−Fe−N(2)	91.14(14)	N(2)−C(6)−C(7)	108.5(4)
N(4)−Fe−N(2)	164.1(2)	C(8)−C(7)−C(6)	107.9(4)
N(3)−Fe−N(2)	93.66(14)	C(7)−C(8)−C(9)	107.0(4)
N(1)−Fe−C(36)	99.1(2)	N(2)−C(9)−C(10)	123.9(4)
N(4)−Fe−C(36)	98.5(2)	N(2)−C(9)−C(8)	110.0(4)
N(3)−Fe−C(36)	96.4(2)	C(10)−C(9)−C(8)	126.2(4)
N(2)−Fe−C(36)	96.1(2)	C(9)−C(10)−C(11)	124.2(4)
C(4)−N(1)−C(1)	108.7(3)	N(3)−C(11)−C(10)	124.0(4)
C(4)−N(1)−Fe	132.4(3)	N(3)−C(11)−C(12)	109.4(4)
C(1)−N(1)−Fe	118.6(2)	C(10)−C(11)−C(12)	126.6(4)
C(9)−N(2)−C(6)	106.5(3)	C(13)−C(12)−C(11)	106.9(4)
C(9)−N(2)−Fe	126.2(3)	C(12)−C(13)−C(14)	108.0(4)
C(6)−N(2)−Fe	126.2(3)	C(15)−C(14)−N(3)	125.0(4)
C(11)−N(3)−C(14)	107.3(3)	C(15)−C(14)−C(13)	126.5(4)
C(11)−N(3)−Fe	126.0(3)	N(3)−C(14)−C(13)	108.4(4)
C(14)−N(3)−Fe	125.9(3)	C(14)−C(15)−C(16)	123.5(4)
C(16)−N(4)−C(19)	108.4(3)	N(4)−C(16)−C(15)	120.4(3)
C(16)−N(4)−Fe	132.9(3)	N(4)−C(16)−C(17)	108.7(3)
C(19)−N(4)−Fe	118.5(2)	C(15)−C(16)−C(17)	130.9(4)
C(19)−C(1)−N(1)	110.6(3)	C(18)−C(17)−C(16)	108.3(3)
C(19)−C(l)−C(2)	141.2(4)	C(17)−C(18)−C(19)	107.0(3)
N(1)−C(1)−C(2)	108.1(3)	C(1)−C(19)−N(4)	111.0(3)
C(3)−C(2)−C(l)	106.6(4)	C(l)−C(19)−C(18)	141.5(4)
C(2)−C(3)−C(4)	108.5(3)	N(4)−C(19)−C(18)	107.5(3)
N(1)−C(4)−C(5)	121.2(3)	C(37)−C(36)−C(41)	120.1(5)
N(1)−C(4)−C(3)	108.1(3)	C(37)−C(36)−Fe	119.5(3)
C(5)−C(4)−C(3)	130.7(4)	C(41)−C(36)−Fe	120.3(4)

[a] Only values for the corrole macrocycle are given. Numbers in parentheses are estimated standard deviations in the least significant digit.

Finally, it should be also noted that many electrogenerated phenyl σ-bonded iron(IV) porphyrins are unstable at room temperature and undergo a phenyl migration from the metal to one of the four nitrogens of the porphyrin ring.[3] Recently, $[(OETPP)Fe^{IV}(C_6H_5)]^+$ was shown to be stable at room temperature,[17] but this is not the case for the electrochemically generated iron(IV) π cation radical $[(OETPP)Fe^{IV}(C_6H_5)]^{\bullet 2+}$, which undergoes a phenyl migration to give the corresponding Fe(III) *N*-phenylporphyrin. The results in this work show that such a reaction does not occur either for the neutral phenyl σ-bonded iron(IV) corrole or for its singly or doubly oxidized products, at least on the cyclic voltammetry time scale. No chemically or electrochemically generated phenyl σ-bonded iron(IV) porphyrins have been sufficiently stable to be crystallography characterized, and to date, the only phenyl σ-bonded iron(IV) tetrapyrrole macrocycle for which an X-ray structure is available is $(OEC)Fe^{IV}(C_6H_5)$.[25] The crystal structures of $(OEC)Fe(C_6H_5)$ and $[(OEC)Fe(C_6H_5)]^{\bullet +}$ show that the Fe−N distance in these complexes is smaller than that in $(TPP)Fe(C_6H_5)$.[49] One might therefore suggest that an overlap of π electrons onto the metal will result in a decrease of electron density on the nitrogen, and this might preclude an *N*-phenyl migration for this type of complex.

Electrochemistry of Iron Corroles As Compared to Iron Porphyrins. A major difference between corroles and porphyrins is the charge of the deprotonated macrocycle (−3 for the corroles and −2 for the porphyrins). This leads to the corroles being easier to oxidize and harder to reduce than the porphyrins and at the same time to the corroles being able to stabilize higher oxidation states of the central metal ion than in the case of the corresponding porphyrins. Quantitatively, the degree of stabilization can be seen from comparisons between half-wave potentials for a given redox process of the two macrocycles, *e.g.* Fe(IV)/Fe(III) or Fe(III)/Fe(II). The difference in $E_{1/2}$ is about 1 V, with the corrole potentials all being shifted toward more negative values. For example, the Fe(IV)/Fe(III) process of $(OEP)Fe^{III}(C_6H_5)$[3] is located at $E_{1/2} = 0.48$ V while the same reaction of $(OEC)Fe^{IV}(C_6H_5)$ occurs at $E_{1/2} = -0.61$ V (see Table 2). A similar $\Delta E_{1/2}$ is observed between the formal Fe(III)/Fe(II) reactions of the same two complexes where the Fe(III) porphyrin[3] is reduced at $E_{1/2} = -0.93$ V and the Fe(III) corrole at $E_{1/2} = -1.98$ V (see Table 2).

Similar comparison in the redox behavior can be made between cobalt[27,50] porphyrins and corroles. For example, the Co(III)/Co(II) reaction of (T-*p*-ClPP)$Co^{II}(PPh_3)$ (where T-*p*-ClPP is the dianion of tetrakis(*p*-chlorophenyl)porphyrin) occurs at $E_{1/2} = +0.30$ V in PhCN[27] while the same redox process of the corresponding triphenylcorrole complex, (OMT-*p*-ClPC)-$Co^{III}(PPh_3)$, occurs at $E_{pc} = -0.89$ V under the same solution conditions.[27]

It is also worth mentioning that the Fe(IV)/Fe(III) process of $[Fe^{IV}Cl(\eta^4\text{-MAC*})]^-$ (where MAC* = a tetraanionic tetraamide ligand) occurs at $E_{1/2} \approx +0.40$ V vs SCE in CH_2Cl_2,[23b] *i.e.*, at a potential which is much more positive than $E_{1/2}$ for the Fe(IV)/Fe(III) process of $(OEC)Fe^{IV}Cl$ ($E_{1/2} = -0.08$ V vs SCE in CH_2Cl_2). Thus, the trianionic corrole ligand seems to provide a stronger stabilizing effect than the tetraanionic tetraamide MAC* macrocycle, where stabilization of the Fe(IV) species is associated only with the large σ-donor capacity of the four amido nitrogens, since this ligand lacks a delocalized π-system.[23b] Therefore, one must conclude that the presence of a large aromatic π-system in the corrole macrocycle is an important factor stabilizing the higher Fe(IV) oxidation state.

An electrochemical comparison between the $(OEC)Fe^{IV}(C_6H_5)$ and $(OEP)Fe^{III}(C_6H_5)$ is shown in Figure 11 and reveals some surprising features. Namely, the oxidations of the two complexes occur at virtually the same potentials, despite different central metal oxidation states. Virtually identical oxidation potentials are also seen for $(OEC)Fe^{III}(NO)$ ($E_{1/2} = +0.61$ V)[26] and $(OEP)Fe^{II}(NO)$ ($E_{1/2} = +0.63$ V)[51] as well as

(47) (a) Renner, M. W.; Barkigia, K. M.; Zhang, Y.; Medforth, C. J.; Smith, K. M.; Fajer, J. *J. Am. Chem. Soc.* **1994**, *116*, 8582. (b) Song, H.; Reed, C. A.; Scheidt, W. R. *J. Am. Chem. Soc.* **1989**, *111*, 6867. (c) Song, H.; Orosz, R. D.; Reed, C. A.; Scheidt, W. R. *Inorg. Chem.* **1990**, *29*, 4274. (d) Scheidt, W. R.; Song, H.; Haller, K. J.; Safo, M. K.; Orosz, R. D.; Reed, C. A.; Debrunner, P. G.; Schulz, C. E. *Inorg. Chem.* **1992**, *31*, 939.
(48) Prendergast, K.; Spiro, T. G. *J. Phys. Chem.* **1991**, *95*, 9728.
(49) Doppelt, P. *Inorg. Chem.* **1984**, *23*, 4009.
(50) Kadish, K. M.; Koh, W.; Tagliatesta, P.; Sazou, D.; Paolesse, R.; Licoccia, S.; Boschi, T. *Inorg. Chem.* **1992**, *31*, 2305.

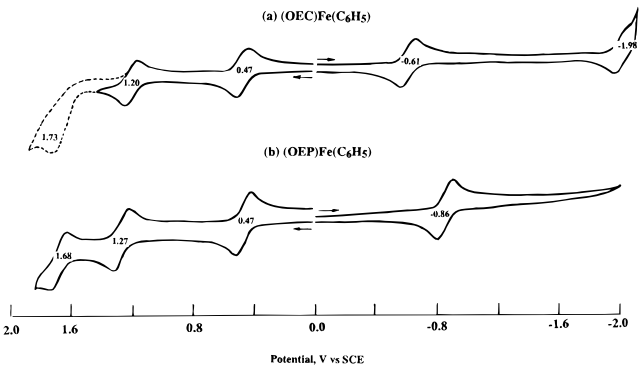

Figure 11. Cyclic voltammograms of (a) (OEC)Fe(C_6H_5) in PhCN, 0.1 M TBAP at a scan rate of 0.1 V/s and (b) (OEP)Fe(C_6H_5) in CH_2Cl_2, 0.2 M TBAP at a scan rate of 0.3 V/s.

for (OMT-*p*-ClPC)$Co^{III}(PPh_3)$ ($E_{1/2} = +0.31$ V)[27] and (T-*p*-ClPP)$Co^{II}(PPh_3)$ ($E_{1/2} = +0.30$ V)[27] in PhCN. This insensitivity toward the metal oxidation state could imply that the abstraction of one electron from these complexes depends only on the overall charge distribution of the molecule or it could be only a coincidence. In this regard it should be pointed out that similar $E_{1/2}$ values are not observed for reduction of the corroles and the porphyrins and that these electrode reactions are sensitive to the central metal oxidation state. This is evidenced by the fact that the first reduction of the three investigated Fe(IV) corroles occurs at $E_{1/2}$ values which are 0.3−0.5 V more positive than $E_{1/2}$ for the same electrode reactions of the corresponding Fe(III) porphyrins (*e.g.*, the first reductions of (OEC)$Fe^{IV}(C_6H_5)$ and (OEP)$Fe^{III}(C_6H_5)$[3] in PhCN occur at $E_{1/2} = -0.61$ V and -0.93 V, respectively).

In summary, the iron corroles are much easier to oxidize than the porphyrins when the same set of redox processes are considered (*e.g.*, Fe(II)/Fe(III) or Fe(III)/Fe(IV)), but the absolute values of $E_{1/2}$ for a given electrooxidation may depend upon the overall charge distribution of the macrocycle rather than upon the oxidation state of the central metal ion.

Acknowledgment. The support of the Robert A. Welch Foundation (K.M.K., Grant E-680) is gratefully acknowledged. We also acknowledge Dr. Naoto Azuma for EPR measurements at 77 K, Dr. E. Bill for Mössbauer data, and Prof. K. Wieghardt for magnetic susceptibility measurements.

Supporting Information Available: Tables containing details of data acquisition and refinement, atomic coordinates and isotropic thermal parameters, bond lengths, bond angles, torsion angles, and anisotropic thermal parameters and an ORTEP plot with complete labeling (18 pages).

IC9509037

(51) (a) Mu, X. H.; Kadish, K. M. *Inorg. Chem.* **1988**, *27*, 4720. (b) Lançon, D.; Kadish, K. M. *J. Am. Chem. Soc.* **1983**, *105*, 5610.

(52) (a) A similar conclusion was also reached by Boschi *et al.*[52b] (b) Licoccia, S.; Paci, M.; Paolesse, R.; Boschi, T. *J. Chem. Soc., Dalton. Trans.* **1991**, 461.